Assessment of the aerosol water content in urban atmospheric particles by the hygroscopic growth measurements in Sapporo, Japan

Yasuyuki Kitamori[1,2], Michihiro Mochida[3], Kimitaka Kawamura[1]

[1] Institute of Low Temperature Science, Hokkaido University, N19 W8, Kita-ku, Sapporo 060-0819, Japan

[2] Graduate School of Earth Environmental Science, Hokkaido University, N10 W5, Kita-ku, Sapporo 060-0810, Japan

[3] Institute for Advanced Research, Nagoya University, Furo-cho, Chikusa-ku, Nagoya 464-8601, Japan

Corresponding author telephone numbers: +81-11-706-7448; fax +81-11-706-7142; e-mail: kitamori@pop.lowtem.hokudai.ac.jp

Abstract

Aerosol water content (AWC) of urban aerosol particles was investigated based on the hygroscopic growth measurements for 100 and 200 nm particles using a hygroscopicity tandem differential mobility analyzer in Sapporo, Japan in July 2006. In most of the humidogram measurements, presence of less and more hygroscopic modes was evident from the different dependence on relative humidity (RH). The volume of liquid water normalized by that of dry particle ($V_w(RH)/V_{dry}$) was estimated from the HTDMA data for 100 and 200 nm particles. The RH dependence of $V_w(RH)/V_{dry}$ was well represented by a fitted curve with a hygroscopicity parameter κ_{eff}. The κ_{eff} values for 200 nm particles were in general higher than those for 100 nm particles, indicating a higher hygroscopicity of 200 nm particles. Based on the κ_{eff} values, the volume mixing ratios of water-soluble inorganic compounds (ammonium sulfate equivalent) were estimated to be on average 31% and 45% for 100 and 200 nm particles, respectively. The diurnal variation of κ_{eff}, with relatively higher values in the noontime and nighttime and lower values in the morning and evening hours, was observed for both particle sizes. The $V_w(RH)/V_{dry}$ values under ambient RH conditions were estimated from κ_{eff} to range from 0.05 to 2.32 and 0.06 to 2.43 for 100 nm and 200 nm particles, respectively. The degree of correlation between κ_{eff} and $V_w(RH)/V_{dry}$ at ambient RH suggests a significant contribution of the variation of κ_{eff} to atmospheric AWC in Sapporo.

Keywords: Atmospheric particles; HTDMA; Particle hygroscopicity; Parameterization; Aerosol water content

1. Introduction

The ability of atmospheric aerosol particles to retain liquid water, i.e., the aerosol hygroscopicity, is closely related to various atmospheric properties and processes. For example, the optical property of aerosols, which affects scattering and absorption of solar radiation, is sensitive to changes in the particle size due to water uptake as a function of relative humidity (RH) (Tang, 1996). The presence of liquid water and its amount in aerosol particles influence aqueous phase chemical reactions (McMurry and Wilson, 1983) and partitioning of semi-volatile compounds between gas and particle phases (Ansari and Pandis, 2000). Furthermore, since the hygroscopic behavior of particles is closely related to the cloud condensation nuclei activity, it determines whether or not a cloud and/or fog droplet is formed under a given supersaturated water vapor condition.

There are several issues that have been studied to better understand the hygroscopic behaviors of aerosol particles. For instance, externally-mixed conditions of aerosols were observed in various locations (McMurry and Stolzenburg, 1989; Zhang et al., 1993; Bush et al., 2002). The relationship of the particle hygroscopicity to the chemical composition has been studied for inorganic salts (e.g., Tang and Munkelwitz, 1994), organic compounds, and organic/inorganic mixtures (e.g., Cruz and Pandis, 2000; Peng et al., 2001; Prenni et al., 2001). The hysteresis of aerosol hygroscopic growth was assessed in field studies (Santarpia et al., 2004), and has been discussed in view of the radiative impact (Martin et al., 2003, 2004). Moreover, the RH dependence of the aerosol optical property has been studied, with various techniques including nephelometer, aerosol lidar, and cavity ring-down aerosol extinction spectrometer (Carrico et al., 2003; Feingold and Morley, 2003; Baynard et al., 2007).

Asia is a region where both anthropogenic and natural emissions of aerosols and their precursors are significant (Huebert et al., 2003), yet hygroscopicity data of atmospheric particles is still scarce. We have investigated the humidity dependence on the water content of

urban atmospheric particles in the Japanese large city Sapporo, based on hygroscopic growth measurements using a hygroscopicity tandem differential mobility analyzer (HTDMA). A single variable parameterization according to κ-Köhler theory (Petters and Kreidenweis 2007) is applied to 100 and 200 nm particles, to assess the degree of the particle hygroscopic growth and the RH dependence, and the general characteristics of the aerosol hygroscopicity in Sapporo in the summer season. Further, the aerosol water content (AWC) under the ambient RH conditions are characterized, and the relative contribution of humidity and particle hygroscopicity to AWC is discussed.

2. Experiments and Data Analyses

2.1. Measurement of aerosol hygroscopic growth

Hygroscopicity of atmospheric aerosol particles was measured using an HTDMA in the Institute of Low Temperature Science (43°05′00″N, 141°20′19″E), Hokkaido University in the city of Sapporo (population: ca. 1.9 million), Japan from 6 to 29 July, 2006. The weather condition was clear and/or cloudy in most of the period, while 11% was rainy. The mean values (ranges) of atmospheric temperature and RH were 21 °C (15–29 °C) and 74% (34–92%) during the observation period, respectively. The HTDMA system (Fig. 1) used in this study is described in Mochida and Kawamura (2004). Here, we briefly explain an outline of the measurement.

Dried and neutralized aerosols were classified into 100 and 200 nm particles (switched every 5 minutes) by the first differential mobility analyzer (DMA1, TSI Model 3081). The monodispersed aerosols were introduced to a prehumidifier (mean ± one standard deviation: 98 ± 1.3% RH, range: 91-99% RH) and RH conditioner (from 9 to 98% RH) and then transferred to the humidified DMA (DMA2) (from 2 to 98% RH) and condensation particle counter (CPC, TSI Model 3010), by which the aerosol hygroscopic growth were measured.

The residence time of particles between the RH conditioner and DMA2 was about 10 s. Flow rates of sample and sheath airs in both DMA1 and DMA2 were 0.3 and 3 L min^{-1}, respectively. The sample air was diluted with filtered air at the inlet of the CPC, and the sample and total air flows were adjusted to 0.3 and 1 L min^{-1}, respectively, using a needle valve (Fig. 1). The RH of the sample aerosol was scanned repeatedly; each cycle required two hours to scan RH from 3 to 97% RH and one hour to dry the system for the next humidogram measurement. In total 186 humidograms were collected.

The performance of the HTDMA was evaluated by the humidogram measurement of the hygroscopic growth of pure $(NH_4)_2SO_4$ particles. The size distribution of humidified particles measured using DMA2 and the CPC in the scanning mobility particle sizer (SMPS) mode was fitted by a Gaussian curve, and the mode of the curve is defined as d(RH). Similarly, dry diameter (d_{dry}) was determined when the RH was below 13% RH during the collection of the humidogram. Here, raw counts data collected in the SMPS mode were converted to the apparent size distribution of particles using the integral of the Stolzenburg DMA transfer function (1988) and a Cunningham slip correction factor of Allen and Raabe (1985). In the case of 100 nm $(NH_4)_2SO_4$ particles, the ratio of d(RH) to d_{dry} (hygroscopic growth factor g(RH)) were 1.25 ± 0.02 and 1.70 ± 0.02 (mean ± one standard deviation, n = 3) at 60 and 90% RH and at 296–297 K, respectively. The values reasonably agree with $g(RH)$ estimated from the literature data of water activity and the density of $(NH_4)_2SO_4$ solution with the consideration of surface tension effect (g = 1.27 at 60% RH and 1.68 at 90% RH at 298K) (Tang and Munkelwitz, 1994). Note that we observed 1% decrease in the mobility diameter of pure $(NH_4)_2SO_4$ particles, with a prehumidification followed by the drying procedure in the HTDMA. This may be due to the restructuring of $(NH_4)_2SO_4$ particles (Gysel et al. 2004). The diameter after the size decrease is defined as a dry diameter of $(NH_4)_2SO_4$ particles.

2.2. Estimate of the aerosol water content of atmospheric particles

The water content of atmospheric particles is assessed using the estimated aerosol water volume $V_w(RH)$ divided by the dry particle volume V_{dry} at <13% RH for aerosols humidified in the HTDMA:

$$AWC \equiv \frac{V_w(RH)}{V_{dry}} = \frac{V(RH) - V_{dry}}{V_{dry}} \quad (1)$$

$$V(RH) = \sum_i N_i(RH) \cdot \frac{\pi}{6} \cdot d_i^3 \quad (2)$$

where V_{dry} and $V(RH)$ are the particle volumes in the aerosols under dried and humidified conditions, respectively. They are calculated from the size distribution measured with 64 bins per decade using DMA2+CPC in the SMPS mode. V(RH) is calculated from Eq. (2), where d_i is the midpoint of the diameter of the size bin i, and N_i(RH) is the particle number concentration within the bin. V_{dry} is calculated from Eq. (2) by substituting d_i to the mode of the Gaussian fitting to the observed dry distribution, as in the case of the growth factor measurement of $(NH_4)_2SO_4$ particles. It is assumed that the particles are spherical and that the amount of residual water in the dried particles is negligible. Further, Eq. (1) assumes that the water volume $V_w(RH)$ is equal to the changes in the volume of aerosol particles with RH, thereby neglecting a change in the partial molar volume of the compounds in a particle.

Because apparent distributions of N_i(RH) determined without an inversion procedure are used for the calculation of V_w(RH)/V_{dry}, broadening of the distribution due to the width of DMA2 transfer function (e.g., Swietlicki et al., 2008) possibly biases V_w(RH)/V_{dry}. We thereby assessed the bias using a forward model with Stolzenburg DMA transfer function (1988). In the model, size distributions of dry particles classified to 100 and 200 nm in DMA1

were calculated from the transfer function, on the assumption of constant dN/dlogd_{dry} of charged particles along d_{dry} upstream of DMA1. Modeled aerosol particles were then grown by factors between 1.002 and 1.778, and the apparent size distributions observed using DMA2+CPC were calculated. The apparent distribution is first calculated in the size resolution of 1024 bins per decade, and next converted to lower resolution (64 bins per decade). Smearing of the transfer function in the SMPS mode (Russell et al., 1995, Collins et al., 2004) was not considered. Fig. 2a presents the differences between the apparent and theoretical V_w(RH)/V_{dry} values estimated by the model. We have found that the relative errors for 100 and 200 nm particle are small in the range of AWC above 0.2, and the errors are mainly from the Gaussian fitting procedure. Fig. 2b and Fig 2c present the apparent size distributions for 100 and 200 nm at the growth factor 1.00 and 1.72 obtained from model calculation as well as those measured under dry RH condition. The apparent size distributions modeled under dry condition well reproduce the measured distribution, supporting the validity of this assessment.

The bias of V_w(RH)/V_{dry} was further found to be small, from the HTDMA measurement using pure $(NH_4)_2SO_4$ particles. The differences in the V_w(RH)/V_{dry} values calculated from Eqs. (1) and (2) and those calculated using the mode growth factor derived from Gaussian fittings were only 3.3 and 2.1% at 60 and 90% RH, respectively. A possible reason for the higher deviation at 60% RH is a faster scan of RH at lower RH, resulting in a larger errors of RH and thus V_w(RH)/V_{dry}.

In the case of atmospheric particles with apparent g(RH) ~ 1, the AWC is possibly underestimated. They probably contain aggregates of black carbon in the urban air, and the mobility diameter measurement of such non-spherical particles is not sensitive to their volume change by the hygroscopic growth (Slowik et al., 2007). Although this point is remained as an open question, we regard that the uncertainty of AWC is not significant if the substantial

fraction of aerosol particles is more hygroscopic (g(RH) > 1) as observed in this study. General agreements on the chemical closure of aerosol hygroscopicity using HTDMA were reported (Dick et al., 2000; Aklilu et al., 2006; Gysel et al., 2007; Aggarwal et al., 2007), which support our assumption.

We predict the AWC of aerosol particles under real atmospheric conditions by applying the ambient RH to the fitted curves of V_w(RH)/V_{dry}. The ambient RH used for the analysis was measured by Sapporo District Meteorological Observatory (43°03′30″N, 141°19′42″E).

2.3. Calculation of hygroscopicity κ from aerosol water content

In this study, the κ-Köhler theory (Petters and Kreidenweis 2007) is used to fit observed V_w(RH)/V_{dry}. The RH in equilibrium with a droplet is given in the theory by:

$$\frac{RH(\%)}{100} = \frac{d^3(RH) - d_{dry}^3}{d^3(RH) - d^3(1-\kappa)} \exp\left(\frac{4\sigma M_w}{RT\rho_w d(RH)}\right), \quad (3)$$

where

$$\kappa = \sum \varepsilon_i \kappa_i . \quad (4)$$

The hygroscopicity of a multi-component particle is represented by κ. In the equations, ρ_w and M_w are the density and the molecular weight of the water, respectively, σ is the surface tension of the solution/air interface, R and T are the gas constant and temperature, respectively, and ε_i and κ_i are the dry volume fractions and the hygroscopicity of compound i.

For the fitting to observed V_w(RH)/V_{dry}, the Kelvin term in Eq. (3) is approximated by a constant

$$A=\exp(4\sigma M_w/RT\rho_w d_{dry}) \quad (5)$$

where the surface tension σ is 0.072 J m^{-2}, T=298.15 K, and d(RH) is substituted with d_{dry}. For the fraction of particles with hygroscopicity κ_j in the aerosol classified by DMA1, the ratio of the water volume ($v_{j,w}$(RH)) and the dry volume ($v_{j,dry}$) of particle in the fractions is derived from Eq. (3):

$$\frac{v_{j,w}(RH)}{v_{j,dry}} = \frac{d_j(RH)^3 - {d_{dry}}^3}{{d_{dry}}^3} \cong \kappa_j \frac{\frac{RH(\%)}{100}}{\left(A - \frac{RH(\%)}{100}\right)}. \quad (6)$$

The $d_j(RH)$ is the diameter of humidified particles with hygroscopicity κ_j. For externally-mixed aerosols with particles with different κ_j, Eq. (6) is extended to:

$$AWC \equiv \frac{V_w(RH)}{V_{dry}} = \frac{\sum_j n_j \left(\frac{v_{j,w}(RH)}{v_{j,dry}}\right)}{\sum_j n_j} \cong \kappa_{eff} \frac{\frac{RH(\%)}{100}}{\left(A - \frac{RH(\%)}{100}\right)} \quad (7)$$

where n_j is the number concentrations of particles with hygroscopicity κ_j, and κ_{eff} is the effective κ for the externally-mixed aerosols. We use κ_{eff} as a fitting parameter to represent AWC as a function of RH.

2.4. Estimation of volume fraction of water-soluble inorganic salts

A two-component model, with water-soluble $(NH_4)_2SO_4$ and water-insoluble components, is used to estimate the volume fraction of water-soluble inorganic salts

(Pitchford and McMurry, 1994). Assuming that κ is zero for insoluble fraction, one can estimate the volume fraction of soluble inorganic salts from the ratio of κ to the hygroscopicity of pure $(NH_4)_2SO_4$ particle κ_{AS}. The κ_{AS} value is derived to be 0.46 from the fitting of the equation:

$$a_w = 1 + \kappa \frac{V_{dry}}{V_w(RH)}. \quad (8)$$

where the water activity a_w and $V_{dry}/V_w(RH)$ are estimated from literature data (Tang and Munkelwitz, 1994), including the density of $(NH_4)_2SO_4$ solution.

3. Results and Discussion

3.1. Hygroscopic growth and liquid water content of aerosol particles

An example of the humidogram measurements for atmospheric aerosol particles in Sapporo is presented in Fig. 3(a). Two hygroscopic modes were observed; one shows an increase in particle diameter with increasing RH (more hygroscopic mode particles), whereas the other does not (less hygroscopic mode particles). Most of the humidograms for both 100 and 200 nm particles showed two modes, although the measured aerosols were occasionally dominated by either less or more hygroscopic mode particles, or moderately hygroscopic mode particles with quasi-unimodal distribution. The results are consistent with the fact that bimodal distributions of particle hygroscopicity are typical in urban environments (e.g. Swietlicki et al., 2008). The hygroscopic growth of more hygroscopic mode particles were lower than that of pure inorganic salts such as $(NH_4)_2SO_4$ and NH_4NO_3 (Fig. 3a). The particles observed in the more hygroscopic mode were probably a mixture of water-soluble inorganic salts and other components such as organics (Saxena et al., 1995). The particles in

the less hygroscopic mode may contain black carbon and non-polar organic substances from primary sources (Zhang et al., 1993).

The $V_w(RH)/V_{dry}$ values of aerosol particles are calculated using Eqs. (1) and (2). The open circles in Fig. 3b are calculated from the data plotted in Fig. 3a. The $V_w(RH)/V_{dry}$ shows a clear increasing trend with increasing RH, as a result of the hygroscopic growth of particles in more hygroscopic mode fraction. The RH dependence of $V_w(RH)/V_{dry}$ was fitted by Eq. (7) using κ_{eff} as a single fitting parameter. The κ_{eff} from the fitting of the measuremnt in Fig. 2b is 0.191 ± 0.007. The κ_{eff} values were obtained for all 186 samples (see section 3.2).

This regression analysis was further applied to the average of $V_w(RH)/V_{dry}$ from 186 measurements. The κ_{eff} derived from the average ($\kappa_{eff,ave}$) for 100 nm particles was 0.141 ± 0.001, whereas that for 200 nm particles was 0.209 ± 0.003 (Fig. 4a). The higher $\kappa_{eff,ave}$ value for larger particles can be explained by the general characteristic of urban aerosols: smaller particles are characterized by elemental carbon and primary anthropogenic organic aerosols which are less water-soluble, while larger particles are dominated by water-soluble secondary organics and inorganics (Allan et al., 2003; Alfarra et al., 2004; Zhang et al., 2005; Takegawa et al., 2006). It should be noted that the k_{eff} values are not significantly affected by the Kelvin effect, because the effect is taken into account outside of k_{eff} in Eq. (3).

Fig. 4b presents the differences between the $V_w(RH)/V_{dry}$ directly calculated from measured g and those indirectly calculated from the regression curves with κ_{eff}. For both 100 and 200 nm particles, the relative errors were very small at high RH (>40% RH), whereas they were larger at low RH (≤40% RH). The overestimation at low RH is probably explained by the efflorescence of aerosol particles and the particle morphology in the dry condition. While our regression analysis has no consideration of the efflorescence of particles, some components such as ammoniated sulfate in particles may crystallize at low RH. The

efflorescences RH (ERH) of $(NH_4)_2SO_4$ and $(NH_4)_3H(SO_4)_2$ is 32.1 ± 2.5% RH at 298 K (Takahama et al., 2007) and 35% RH at 298 K (Martin, 2000), respectively, which agree with the range of large relative errors in Fig. 4b. In addition, given that dry particles are slightly non-spherical or porous and that they are spherical after humidification, the use of mobility diameter instead of volume-equivalent diameter for dry particles in Eq. (2) leads to an underestimation of V_w (RH)/V_{dry} in particular at low RH. If the dynamic shape factor χ of dry particles of 1.04 (the value reported for $(NH_4)_2SO_4$ by Zelenyuk et al. (2006)) is applied, the associated error is from –95 to –45% at <40% RH, which well explains the magnitude of errors in Fig. 4b.

3.2. Particle hygroscopicity and the volume fraction of water-soluble inorganic salts

Fig. 5a and b shows histograms of κ_{eff} obtained from the regression analysis of 186 samples for 100 and 200 nm particles, respectively. A large variability of κ_{eff} is evident. The κ_{eff} values for 100 nm particles ranged from 0.026 to 0.321 with a mean (median) of 0.142 (0.133). For 200 nm particles, it ranged from 0.027 to 0.494 with a mean (median) of 0.209 (0.205). Not only the average of κ_{eff} but also the relative standard deviation for 200 nm particles (0.089) is larger than that of 100 nm particles (0.065). It suggests a different degree of the temporal changes in the composition, depending on the dry particle size.

The volume fraction of water-soluble inorganic salts in the particles was estimated by the two-component model (section 2.4), and is shown in the upper *x*-axis in Fig. 5. While the volume fraction of inorganic salts for 100 nm particles ranged from 6 to 70% with a mean (median) of 31% (29%), those for 200 nm particles were higher, ranging from 6% to 107% with a mean (median) of 45% (45%). The mean values of the estimated volume fraction of inorganic salts and the size dependence are similar to those of urban aerosol types

summarized by Kandler and Schütz (2007).

The estimated inorganic salt fraction includes an error associated with the water activity dependence of κ_{AS}. The κ_{AS} values in the range of a_w from 0.8 to 0.95 are 0.42–0.57, which leads to relative errors up to 26% in the estimated volume fraction. Further, the estimate also depends on the choice of compound for soluble fraction. If $(NH_4)HSO_4$ (κ= 0.59 for a_w<0.95) instead of $(NH_4)_2SO_4$ is used as a model compound, the difference in the estimated fraction of inorganic salt is calculated to be 22%. It should be emphasized that the magnitude of these errors is significantly smaller than the variation of soluble fraction in Fig. 5.

3.3. Diurnal variation of the particle hygroscopicity

Fig. 6 shows the diurnal variation of κ_{eff} during the observation period. The κ_{eff} of 200 nm particles gradually increased from the morning (05-07 LT) to noon (11-13 LT). In the afternoon it gradually decreased, and then increased again from late-evening (23-01 LT) to early-morning (02-04 LT). The diurnal variation of κ_{eff} for 100 nm was similar. The observed lower κ_{eff} in the morning and the evening is possibly caused by a stronger contribution of combustion particles such as black carbon and organics emitted directly from local primary sources (e.g., motor vehicle exhausts). Since aerosol hygroscopicity has a tendency to increase from urban through continental-polluted to remote areas (McFiggans et al., 2006), the higher κ_{eff} between late-evening and early-morning could be explained by lower contribution of local sources and thus relatively larger contribution of background aged aerosols transported from outside Sapporo.

The peak of κ_{eff} around noontime might be associated with lower rates of primary emissions and enhanced convection, which reduces the relative contribution of less hygroscopic primary particles and enhance the contribution of background aged aerosols. On

the other hand, the contribution of secondary aerosol formation to the peak at noontime is not clear. In daytime, formation of secondary aerosol component may be enhanced, but the effect on the hygroscopicity depends on whether ammoniated sulfate and water-soluble organic compounds are produced more. In Tokyo, reduction of particle hygroscopicity was observed in daytime (Mochida et al., 2008), being opposite to the result in Fig. 6. The absence of the strong size dependence of the diurnal variation in Fig. 6 suggests that the secondary processes, whose effect depends on the surface/volume ratio of the particles, were not significant. More studies, e.g., those on aerosol chemical composition and weekday/weekend effect of emissions, are necessary to clarify this point in the future.

Note that one standard deviation of κ_{eff} in Fig. 6 is larger than that of the magnitude of the diurnal variation. Therefore, factors other than those explained above may control the variation of κ_{eff}, too. Changes in the concentration levels of aged background aerosols (e.g., those from Asian continent), and the non-diurnal variations of their mixing with locally released/formed aerosols may be important, too.

3.4. Aerosol water content under ambient RH conditions

The $V_{\mathrm{w}}(\mathrm{RH})/V_{\mathrm{dry}}$ of 100 and 200 nm particles under ambient RH conditions (RH_{a}) were estimated on the assumption that these particles were present as meta-stable aqueous droplet in the atmosphere (Fig. 7). Although it is a hypothetical case, this simplification is reasonable, because a significant fraction of more hygroscopic particles with hygroscopic growth hysteresis has been reported to exist as supersaturated droplets (Santarpia et al., 2004).

Fig. 7a presents a histogram of the averaged ambient RH during each measurement of the humidogram. The RH in the atmosphere widely ranged from 38 to 92% with a mean (median) of 74% (76%). The RH values were applied to the κ_{eff} calculated by the fitting (Fig. 3b), and then AWC under ambient RH ($V_{\mathrm{w}}(RH_{\mathrm{a}})/V_{\mathrm{dry}}$) was estimated. It should be noted that

the residuals of the fitting are generally insignificant in the atmospheric RH range studied (Fig. 4b). The relative frequency distributions of $V_w(RH_a)/V_{dry}$ clustered in the lower end of the range (see Fig. 7d and 7e). For 100 nm particles, $V_w(RH_a)/V_{dry}$ ranged from 0.05 to 2.32 with a mean (median) of 0.49 (0.34) (Fig. 7d). The $V_w(RH_a)/V_{dry}$ values for 200 nm particles (Fig. 7e) were higher, which ranged from 0.06 to 2.43 with a mean (median) of 0.72 (0.58). The mode peak of distribution was at 0.1–0.2 bins for 100 nm particles (Fig. 7d), whereas it was slightly higher for 200 nm particles (0.3–0.4 bins, Fig. 7e).

According to the theoretical relationship in Eq. (8), $V_w(RH_a)/V_{dry}$ are controlled by both κ_{eff} and RH_a. As seen in Fig. 7b and 7c, While the $V_w(RH_a)/V_{dry}$ shows a strong dependence on the ambient RH, a large variation in $V_w(RH_a)/V_{dry}$ is seen even under similar RH conditions. For example, within a narrow humidity range from 80 to 82.5% RH, the $V_w(RH_a)/V_{dry}$ for 100 nm particles varied from 0.13 to 1.17. This result suggests that the variation in the aerosol hygroscopicity as well as that in the atmospheric RH significantly contribute the variation in the AWC in Sapporo atmosphere.

The relative contributions of κ_{eff} and RH_a to the variation in $V_w(RH_a)/V_{dry}$ are assessed quantitatively from the magnitude of R^2, where R is correlation coefficient between $V_w(RH_a)/V_{dry}$ and two variables. For 100 nm particles, the R^2 of κ_{eff} versus $V_w(RH_a)/V_{dry}$ (0.54) is similar to that of RH versus $V_w(RH_a)/V_{dry}$ (0.44). This result is interpreted that the variation of κ_{eff} contributes to that of $V_w(RH_a)/V_{dry}$ nearly in the same magnitude of that of ambient RH. The relative contribution of κ_{eff} is also significant in the case of 200 nm particles; R^2 of κ_{eff} versus $V_w(RH_a)/V_{dry}$ is 0.29 whereas that of RH versus $V_w(RH_a)/V_{dry}$ is 0.46. It should be noted that κ and RH_a have no correlations (R^2: 0.04 and 0.01 for 100 and 200 nm particles, respectively) and that the κ_{eff} and ambient RH are thus nearly independent variables.

The above results imply that, to assess the contribution of AWC to the aerosol properties

such as light extinction, information on the temporal variation of the hygroscopicity κ is as important as that of ambient RH, at least in the case of urban aerosols similar to that we observed in Sapporo. Therefore, characterization of κ using an HTDMA or similar measurement systems is important in order to obtain/assess input parameters to atmospheric aerosol models dealing with aerosol liquid water content and the related properties.

4. Conclusion

The humidograms of 100 and 200 nm particles were measured using an HTDMA system in Sapporo city on July 2006. More and less hygroscopic modes were both observed in many cases of the humidogram measurement, and the RH dependence of the calculated $V_w(RH)/V_{dry}$ (normalized aerosol water content) of aerosol particles was successfully fitted with a single hygroscopicity parameter κ_{eff}. While κ_{eff} for 100 nm particles ranged from 0.026 to 0.321, κ_{eff} for 200 nm particles was higher (0.027 to 0.494). The size dependence of κ_{eff} indicates that 200 nm particles retain more liquid water than 100 nm particles per unit of dry volume, which may be associated with the chemical composition (Raoult effect). The mean volume fractions (± one standard deviation) of water-soluble inorganic salts estimated using κ_{eff} for 100 and 200 nm particles were 31 (± 14)% and 45 (± 19)%, respectively. In both cases of 100 and 200 nm particles, κ_{eff} was higher on average in noontime and late-evening to early-morning, whereas they were lower in the morning and evening hours. This diurnal pattern may be related to those of local emissions of aerosol particles, and the mixing of locally emitted and long-range transported aerosols.

The normalized aerosol water content under the ambient RH conditions during the observation period were estimated for 100 and 200 nm particles. The $V_w(RH)/V_{dry}$ values for 100 and 200 nm ranged from 0.05 to 2.32 with a mean of 0.49, and from 0.06 to 2.43 with a

mean of 0.72, respectively. It has been revealed that not only the variation of RH but also that of κ_{eff} significantly contributes the variation of aerosol water content for both sizes in the atmosphere. This suggests the importance of understanding the variation in the chemical composition of aerosol particles to infer the RH dependence of the hygroscopic growth and the relevant aerosol properties such as the optical property.

Acknowledgements

This study is in part supported by the Japanese Ministry of Education, Culture, Sports, Science and Technology (MEXT) through grant-in-aid No. 14204055 and 19204055, Northern Advancement Center for Science & Technology, and ASAHI BREWERIES FOUNDATION in Japan. This study was also supported by the Program for Improvement of Research Environment for Young Researchers from Special Coordination Funds for Promoting Science and Technology (SCF) sponsored by MEXT.

References

Aggarwal, S.G., Mochida, M., Kitamori, Y., Kawamura, K., 2007. Chemical closure study on hygroscopic properties of urban aerosol particles in Sapporo, Japan. Environmental Science and Technology 41, 6920-6925.

Aklilu, Y., Mozurkewich, M., Prenni, A.J., Kreidenweis, S.M., Alfarra, M.R., Allan, J.D., Anlauf, K., Brook, J., Leaitch, W.R., Sharma, S., Boudries, H., Worsnop, D.R., 2006. Hygroscopicity of particles at two rural, urban influenced sites during Pacific 2001: Comparison with estimates of water uptake from particle composition. Atmospheric Environment 40, 2650-2661.

Alfarra, M.R., Coe, H., Allan, J.D., Bower, K.N., Boudries, H., Canagaratna, M.R., Jimenez, J.L., Jayne, J.T., Garforth, A.A., Li, S.-M., Worsnop, D.R., 2004. Characterization of urban and rural organic particulate in the Lower Fraser Valley using two Aerodyne Aerosol Mass Spectrometers. Atmospheric Environment 38, 5745-5758.

Allan, J.D., Alfarra, M.R., Bower, K.N., Williams, P.I., Gallagher, M.W., Jimenez, J.L., McDonald, A.G.., Nemitz, E., Canagaratna, M.R., Jayne, J.T., Coe, H., Worsnop D.R., 2003. Quantitative sampling using an Aerodyne aerosol mass spectrometer 2. Measurements of fine particulate chemical composition in two U.K. cities. Jouranl of Geophysical Research 108 (D3), doi:10.1029/2002JD002359.

Allen, C.M., Raabe, O.G., 1985. Slip correction measurements of spherical solid aerosol particles in an improved Millikan apparatus. Aerosol Science and Technology 4, 269-286.

Ansari, A.S., Pandis, S.N., 2000. The effect of metastable equilibrium states on the partitioning of nitrate between the gas and aerosol phase. Atmospheric Environment 34, 157-168.

Baynard, T., Lovejoy, E.R., Pettersson, A., Brown, S.S., Lack, D., Osthoff, H., Massoli, P., Ciciora, S., Dube, W.P., Ravishankara, A.R., 2007. Design and application of a pulsed

cavity ring-down aerosol extinction spectrometer for field measurements. Aerosol Science and Technology 41, 447-462.

Bush, B., Kandler, K., Schütz, L., Neusüβ, C., 2002. Hygroscopic properties and water-soluble volume fraction of atmospheric particles in the diameter range from 50 nm to 3.8 μm during LACE 98. Journal of Geophysical Research 107 (D21) D218119, doi:10.1029/2000JD000228.

Carrico, C.M., Kus, P., Rood, M.J., Quinn, P.K., Bates, T.S., 2003. Mixtures of pollution, dust, sea salt, and volcanic aerosol during ACE-Asia: Radiative properties as a function of relative humidity. Journal of Geophysical Research 108 (D23) 8650, doi:10.1029/2003JD003405.

Collins, D.R., Cocker, D.R, Flagan, R.C., Seinfeld, J.H., 2004. The scanning DMA transfer function, Aerosol Science and Technology, 38, 833-850.

Cruz, C.N., Pandis, S.N., 2000. Deliquescence and hygroscopic growth of mixed inorganic-organic atmospheric aerosol. Environmental Science and Technology 34, 4313-4319.

Dick, W.D., Saxena, P., McMurry, H.P., 2000. Estimation of water uptake by organic compounds in submicron aerosols measured during the Southeastern Aerosol and Visibility Study. Journal of Geophysical Research 105 (D1), 1471-1479.

Feingold, G., Morley, B., 2003. Aerosol hygroscopic properties as measured by lidar and comparison with in situ measurements. Journal of Geophysical Research 108 (D11) 4327, doi:10.1029/2002JD002842.

Gysel, M., Weingartner, E., Nyeki, S., Paulsen, D., Baltensperger, U., Galambos, I., Kiss, G.., 2004. Hygroscopic properties of water-soluble matter and humic-like organics in atmospheric fine aerosol. Atmospheric Chemistry and Physics 4, 35-50.

Gysel, M., Crosier, J., Topping, D.O., Whitehead, J.D., Bower, K.N., Cubison, M.J., Williams,

P.I., Flynn, M.J., McFiggans, G.B., Coe, H., 2007. Closure study between chemical composition and hygroscopic growth of aerosol particles during TORCH2. Atmospheric Chemistry and Physics 7, 6131-6144.

Huebert, B.J., Bates, T., Russell, P.B., Shi, G., Kim, Y.J., Kawamura, K., Carmichael, G., Nakajima, T., 2003. An overview of ACE-Asia: Strategies for quantifying the relationships between Asian aerosols and their climatic impacts, Journal of Geophysical Research 108(D23), 8633, doi:10.1029/2003JD003550.

Kandler, K., Schütz, L., 2007. Climatology of the average water-soluble volume fraction of atmospheric aerosol. Atmospheric Research 83, 77-92.

Martin, S.T., 2000. Phase transitions of aqueous atmospheric particles. Chemical Reviews 100, 3403-3453.

Martin, S.T., Schlenker, J.C., Malinowski, A., Hung, H.-M., Rudich, Y., 2003. Crystallization of atmospheric sulfate-nitrate-ammonium particles. Geophysical Research Letters 30 (21) 2102, doi:10.1029/2003GL017930.

Martin, S.T., Hung, H.-M., Park, R.J., Jacob, D.J., Spurr, R.J.D., Chance, K.V., Chin, M., 2004. Effects of the physical state of tropospheric ammonium-sulfate-nitrate particles on global aerosol direct radiative forcing. Atmospheric Chemistry and Physics 4, 183-214.

McFiggans, G., Artaxo, P., Baltensperger, U., Coe, H., Facchini, M.C., Feingold, G., Fuzzi, S., Gysel, M., Laaksonen, A., Lohmann, U., Mentel, T.F., Murphy, D.M., O'Dowd, C.D., Snider, J.R., Weingartner, E., 2006. The effect of physical and chemical aerosol properties on warm cloud droplet activation. Atmospheric Chemistry and Physics 6, 2593-2649.

McMurry, H.P., Wilson, J.C., 1983. Droplet phase (heterogeneous) and gas phase (homogeneous) contributions to secondary ambient aerosol formation as functions of relative humidity. Journal of Geophysical Research 88, 5101-5108.

McMurry, P.H., Stolzenburg, M.R., 1989. On the sensitivity of particle size to relative

humidity for Los Angeles aerosols. Atmospheric Environment 23 (2), 497-507.

Mochida, M., Kawamura, K., 2004. Hygroscopic properties of levoglucosan and related organic compounds characteristic to biomass burning aerosol particles. Journal of Geophysical Research 109 (D21202), doi:10.1029/2004JD004962.

Mochida, M., Miyakawa, T., Takegawa, N., Morino, Y., Kawamura, K., Kondo, Y., 2008. Significant alteration in the hygroscopic properties of urban aerosol particles by the secondary formation of organics. Geophysical Research Letters 35 (L02804), doi:10.1029/2007GL031310.

Peng, C., Chan, M.N., Chan, C.K., 2001. The hygroscopic properties of dicarboxylic and multifunctional acids: Measurements and UNIFAC predictions. Environmental Science and Technology 35, 4495-4501.

Petters, M.D., Kreidenweis, S.M., 2007. A single parameter representation of hygroscopic growth and cloud condensation nucleus activity. Atmospheric chemistry and Physics 7, 1961-1971.

Pitchford, M.L., McMurry, P.H., 1994. Relationship between measured water vapor growth and chemistry of atmospheric aerosol for Grand Canyon, Arizona, in winter 1990. Atmospheric Environment 28, 827-839.

Prenni, A.J., DeMott, P.J., Kreidenweis, S.M., Sherman, D.E., Russell, L.M., Ming, Y., 2001. The effects of low molecular weight dicarboxylic acids on cloud formation. Journal of Physical Chemistry A 105, 11240-11248.

Russell, L.M., Flagan, R.C., Seinfeld, J.H., 1995. Asymmetric instrument response resulting from mixing effects in accelerated DMA-CPC measurements, Aerosol Science and Technology, 491-509.

Santarpia, J.L., Li, R., Collins, D.R., 2004. Direct measurement of the hydration state of ambient aerosol populations. Journal of Geophysical Research 109 (D18209),

doi:10.1029/2004JD004653.

Saxena, P., Hildemann, L.M., McMurry, P.H., Seinfeld, J.H., 1995. Organics alter hygroscopic behavior of atmospheric particles. Journal of Geophysical Research 100 (D9), 18755-18770.

Slowik, J.G., Cross, E.S., Han, J.-H., Kolucki, J., Davidovits, Paul., Williams, L.R., Onasch, T.B., Jayne, J.T., Kolb, C.E., Worsnop, D.R., 2007. Measurements of morphology changes of fractal soot particles using coating and denuding experiments: Implications for optical absorption and atmospheric lifetime. Aerosol Science and Technology 41, 734-750.

Stolzenburg M., 1988. An ultrafine aerosol size distribution measuring system. Ph.D. thesis, Department of Mechanical Engineering, University of Minnesota, Minnesota.

Swietlicki, E., Hansson, H.-C., Hämeri, K., Svenningsson, B., Massling, A., McFiggans, G., McMurry, P.H., Petäjä, T., Tunved, P., Gysel, M., Topping, D., Weingartner, E., Baltensperger, U., Rissler, J., Wiedensohler, A., Kulmala, M., 2008. Hygroscopic properties of submicrometer atmospheric aerosol particles measured with H-TDMA instruments in various environments – a review. Tellus Series B-Chemical and Physical Meteorology 60(3), 432-469.

Takegawa, N., Miyakawa, T., Kondo, Y., Jimenez, J.L., Zhang, Q., Worsnop D.R., Fukuda, M., 2006. Seasonal and diurnal variations of submicron organic aerosol in Tokyo observed using the Aerodyne aerosol mass spectrometer. Journal of Geophysical Research 111 (D11206), doi:10.1029/2005JD006515.

Takahama, S., Pathak, R.K., Pandis, S.N., 2007. Efflorescence transitions of ammonium sulfate particles coated with secondary organic aerosol. Environmental Science and Technology 41 (7), 2289-2295.

Tang, I.N., Munkelwitz, H.R., 1994. Water activities, densities, and refractive indices of aqueous sulfates and sodium nitrate droplets of atmospheric importance. Journal of

Geophysical Research 99 (D9), 18801-18808.

Tang, I.N., 1996. Chemical and size effects of hygroscopic aerosols on light scattering coefficients. Journal of Geophysical Research 101 (D14), 19245-19250.

Zelenyuk, A., Cai, Y., Imre, D., 2006. From agglomerates of spheres to irregularly shaped particles: Determination of dynamic shape factors from measurements of mobility and vacuum aerodynamic diameters. Aerosol Science and Technology 40, 197-217.

Zhang, Q., Canagaratna, M.R., Jayne, J.T., Worsnop, D.R., Jimenez, J.L., 2005. Time- and size-resolved chemical composition of submicron particles in Pittsburgh: Implications for aerosol sources and processes. Journal of Geophysical Research 110 (D07S09), doi:10.1029/2004JD004649.

Zhang, X.Q., McMurry, P.H., Hering, S.V., Casuccio, G.S., 1993. Mixing characteristics and water content of submicron aerosols measured in Los Angeles and at the Grand Canyon. Atmospheric Environment 27A (10), 1593-1607.

Figure captions

Fig. 1. Schematic diagram of the hygroscopicity tandem differential mobility analyzer (HTDMA) system.

Fig. 2. (a) Model-derived relative error in apparent $V_w(\mathrm{RH})/V_{dry}$ versus the theoretical $V_w(\mathrm{RH})/V_{dry}$. The solid and dotted lines represent the error for 100 and 200 nm particles, respectively. The apparent $V_w(\mathrm{RH})/V_{dry}$ is calculated using the apparent size distributions with 64 bins per decade, whereas the theoretical $V_w(\mathrm{RH})/V_{dry}$ is equal to $g^3 - 1$. The error was calculated down to the theoretical $V_w(\mathrm{RH})/V_{dry}$ of 4.62. (b) Solid lines: modeled apparent size distributions of particles classified at 100 nm in DMA1, and with growth factor of 1.00 and 1.72. Circles: the apparent dry size distribution measured for pure $(NH_4)_2SO_4$ particles classified at 100 nm in DMA1. (c) Same as (b), but for 200 nm particles.

Fig. 3. (a) An example of the RH dependence of the size distribution of particles after humidification, for particles whose dry diameter was 100 nm (1700-1900 LT on July 8). The particle concentration, represented by the color, is normalized by the total particle number concentrations in the range of the diameter studied. The solid and dashed lines represent diameter changes of $(NH_4)_2SO_4$ and NH_4NO_3 particles estimated from literature data (Tang and Munkelwitz, 1994; Tang, 1996). (b) The aerosol water content normalized by the dry particle volume ($V_w(RH)/V_{dry}$) for the aerosol sample in Fig. 2a. The measurement data (open circles) an the curve fitted with Eq. (7) (solid line) are presented.

Fig. 4. (a) Averaged $V_w(RH)/V_{dry}$ from 186 humidograms. The averaged $V_w(RH)/V_{dry}$ at 5%

RH intervals (open circles: 100 nm particles, open squares: 200 nm particles) are calculated by the interpolation of $V_w(RH)/V_{dry}$ derived from measurements of g for individual humidogram measurement, followed by the averaging of 186 samples. Solid and dotted lines represent the fitted curve with Eq. (8), for 100 and 200 nm particles, respectively. The bars with narrower and wider caps show one standard deviation of the values for 100 and 200 nm particles, respectively. (b) Residual errors between the measured (y) and parameterized ($\hat{y}$) $V_w(RH)/V_{dry}$ calculated by $(y - \hat{y})/\hat{y} \times 100$.

Fig. 5. Histograms of κ_{eff} for (a) 100 nm and (b) 200 nm particles. The upper x-axis shows the volume fraction of inorganic salts in dry particles, which are estimated using the two-component model (see section 2-4).

Fig. 6. Diurnal variations of κ_{eff} for 100 nm (white bar) and 200 nm (grey bar) particles. The sections in the x-axis are the time when the humidograms were measured during the scan from low toward high RH. Mean values in the time sections are presented with the one standard deviation.

Fig. 7. (a) The histogram of the averaged RH in the atmosphere (RH_a) during the measurement of each humidogram. (b) Plots of $V_w(RH)/V_{dry}$ at ambient RH ($V_w(RH_a)/V_{dry}$) against RH_a for 100 nm. (c) Same as (b), but for 200 nm particles. (d) The histogram of $V_w(RH_a)/V_{dry}$ for 100 nm particles. (e) Same as (d), but for 200 nm particles.

Fig. 1. Kitamori et al.

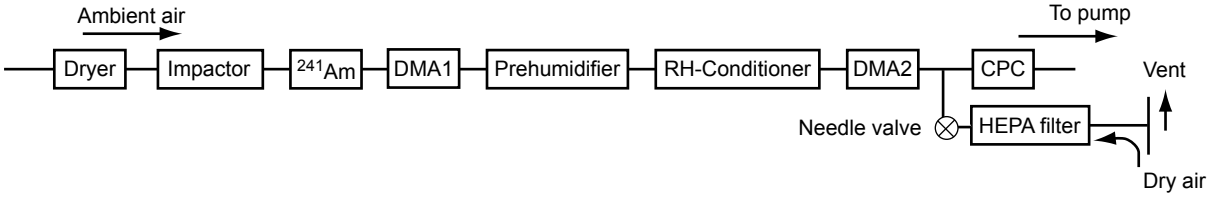

Fig. 2 Kitamori et al.

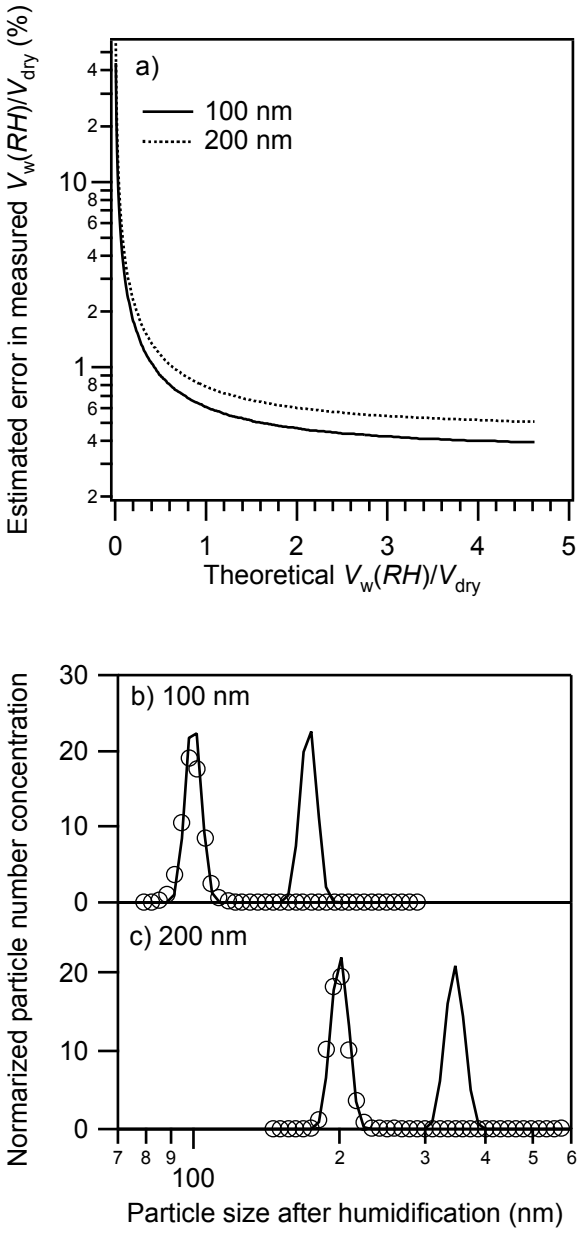

Fig. 3 Kitamori et al.

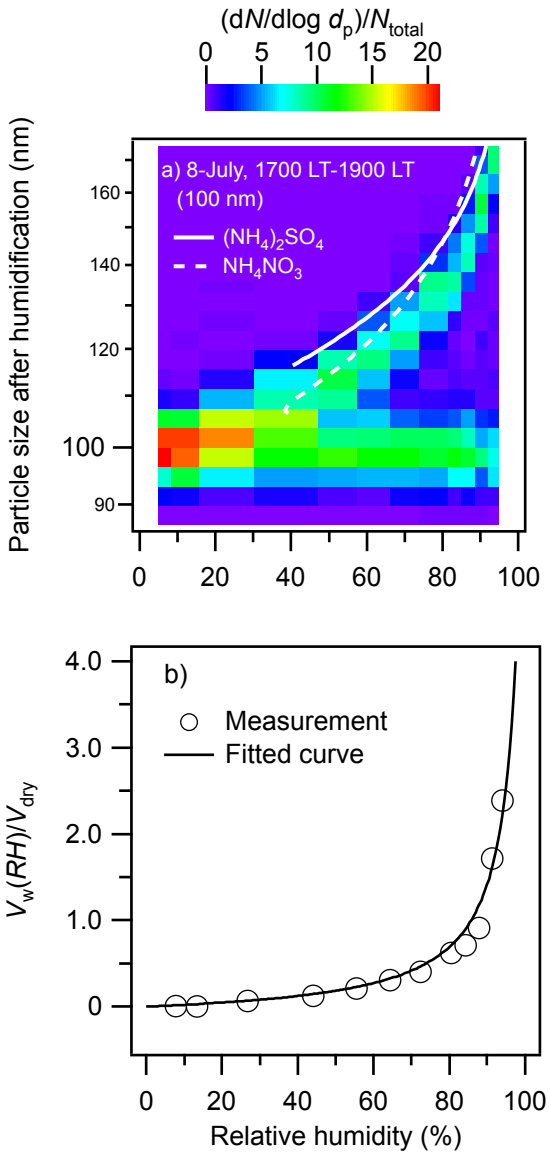

Fig. 4 Kitamori et al.

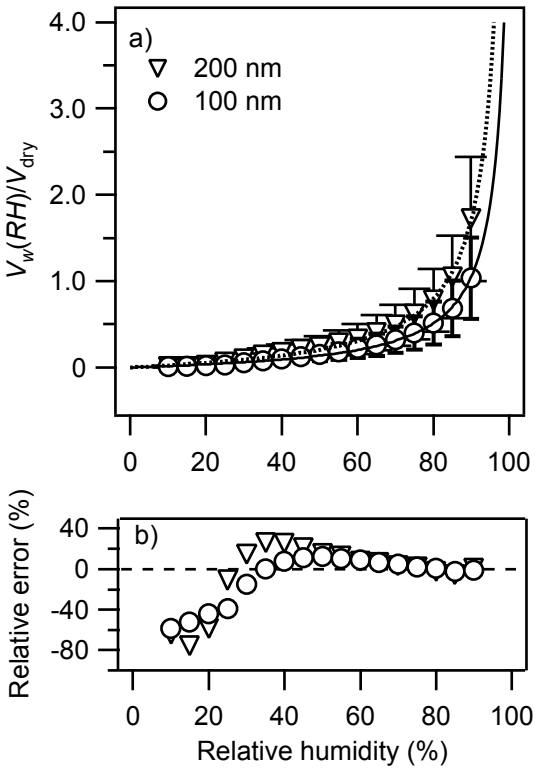

Fig. 5 Kitamori et al.

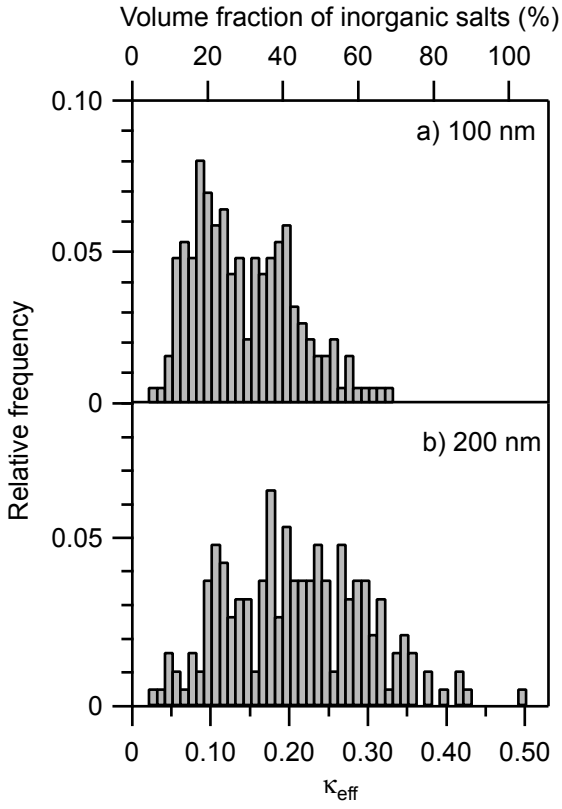

Fig. 6 Kitamori et al.

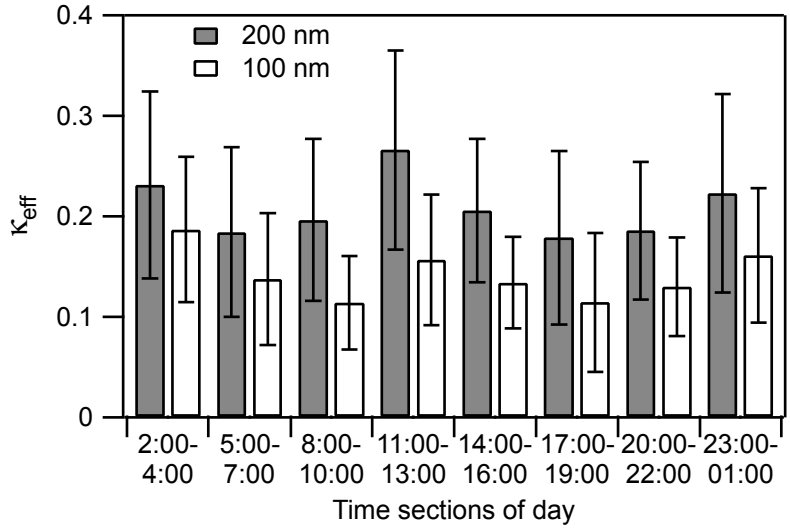

Fig. 7 Kitamori et al.